

Victoria's Secret Problem: Heat Loss in Mastectomy Patients

Keywords: Mastectomy, breast reconstruction, breast implants, heat loss, thermal comfort
MAE 4530/5530: Computer-Aided Engineering | Applications to Biological Processes
© Hsin Huei Chen, Kelly Irons, Taehee Lee, Shubham Mathur May 2022

Table of Contents

1. EXECUTIVE SUMMARY

| | |
|---|-------------------------------------|
| 2. INTRODUCTION | 3 |
| 2.1 Background | 3 |
| 2.2 Problem Statement | 4 |
| 2.3 Design Objectives | 4 |
| 3. METHODS | 4 |
| 3.1 Assumptions | 5 |
| 3.2 Schematic | 6 |
| 3.3 Governing Equations | 7 |
| 3.4 Boundary Conditions | 7 |
| 4. RESULTS | 9 |
| 4.1 Mesh Convergence Analysis | 9 |
| 4.2 Objective Function | 10 |
| 4.3 Temperature Distribution | 10 |
| 4.4 Sensitivity Analysis | 11 |
| 4.5 Validation | 13 |
| 5. DISCUSSION | 16 |
| 6. CONCLUSION | 16 |
| APPENDIX I: Model Input Parameters | 18 |
| APPENDIX II: Generation of Breast Geometry | 21 |
| APPENDIX III: Solution Strategy | 21 |
| APPENDIX IV: Sensitivity Analysis Plots | 23 |
| APPENDIX V: Solution Strategy | Error! Bookmark not defined. |
| REFERENCES | 25 |

1. EXECUTIVE SUMMARY

Mastectomies are performed to treat or prevent the risk of breast cancer. Annually, over 100,000 women in the US undergo some form of mastectomy [1]. Approximately 40% of women who undergo mastectomies elect to undergo breast reconstruction surgery [2]. Tissue removal during mastectomy decreases insulation and breast reconstruction has been shown to be associated with relatively permanent decreased touch and temperature sensibility at the skin. As a result of these factors, patients are susceptible to thermal injury when attempting to warm their breasts, sometimes even leading to partial and full thickness burns.

The objective of this study was to determine the fabric material and thickness required for an insulating bra that will prevent patients from experiencing excessive heat loss and the associated cold/pain sensations in their breasts at cool room temperature. We determined these parameters by assessing which combinations restored tissue temperatures seen in the reconstructed breast closer to tissue temperatures seen in the natural breast. This heat transfer analysis was performed with geometry based on a representation of the statistical average breast given by the Regensburg Breast Shape Model from the Regensburg University of Applied Sciences. Two breast models were created for comparison: one for the natural breast, with layers for muscle, breast tissue, subcutaneous fat, and skin; and one for the reconstructed breast with layers for implant, muscle, subcutaneous fat, and skin.

The results of this study suggest thicknesses for different bra fabric materials, as well as the potential for designing a safe active heating element. Because the study was conducted with the statistical average breast geometry, these results can be generalized - with caution - to design insulating bras for the general patient population. It would be prudent to further analyze the sensitivity of results to variations in the breast geometry and tissue properties for such future design efforts.

2. INTRODUCTION

2.1 Background

Mastectomies are performed to treat or prevent the risk of breast cancer. Annually, over 100,000 women in the US undergo some form of mastectomy [1]. Approximately 40% of women who undergo mastectomies elect to undergo breast reconstruction surgery [2]. Some studies have shown that, with autogeneous breast reconstruction (i.e., reconstruction using tissue from a different part of the patient's body) patients may suffer from thermoregulation complications in the transplanted tissue [3]. Additionally, the tissue removal process also causes a reduction in sensitivity from decreased insulation to retain body heat, leaving patients often complaining about feeling cold. When seeking to remedy that through heating elements, such as a heating

pad, the combined effects of decreased sensitivity and insulation leaves patients more susceptible to thermal injuries (i.e. partial and full thickness burns) [4].

Current research has yet to show how much heat loss occurs due to breast reconstruction compared to normal breasts. Investigating the differences between reconstructed and normal breasts will allow researchers to gain insight on patients' cold sensitivity symptoms, and eventually how to design better insulating materials for patients.

We designed this following study utilizing the Regensburg Breast Shape Model, the Bioheat equation, and reasonable boundary conditions to simulate the heat loss after breast reconstruction.

2.2 Problem Statement

After a mastectomy, patients often complain about feeling cold and losing sensation in their breasts. This sometimes compels them to place hot objects on their skin, leading to burns. It is well known that thermal dysregulation can occur after a mastectomy due to less natural insulation in the form of body fat as well as loss of sensation from transplanted skin. This study aims to optimize the clothing type and thickness that would effectively insulate mastectomy patients. This goal will be achieved by quantifying how much heat is lost in regular and post-mastectomy breasts and selecting a thickness of the clothing that leads to a similar heat loss to the pre-mastectomy breast.

2.3 Design Objectives

The design objective of this study is to choose clothing material(s) and thickness to optimize the enhanced heat loss experienced by mastectomy patients. In order to meet this objective, we will develop a bioheat transfer model for heat loss from the breasts of mastectomy patients under typical indoor environmental conditions using a realistic breast geometry with an added external layer of insulating clothing material. The thickness of the clothing layer will be modified to keep the temperature at the location of temperature receptors within a comfort range. The development of this model will help us understand how the clothing materials and thicknesses affect heat loss and allow us to make informed decisions for future physical proof-of-concept experiments. Other considerations we must take into account when making final recommendations for the design include: economic viability of the bra, which should be made of materials that allow the bra to be affordable for patients; comfort of the bra at the fabric-skin interface; durability of the bra, especially in regard to washing/laundrying; and feasibility of manufacturing the bra.

3. METHODS

3.1 Assumptions

Several assumptions are made for the geometry in order to simplify the breast model. Each of the layers of tissues - skin (combined epidermis, dermis), subcutaneous fat, and muscle - are assumed to be homogenous. The tissue boundaries between tissue layers are assumed to be smooth, not irregular as in actual breast anatomy. In the “normal breast” model (for comparative analysis), breast tissue is treated as one homogenous tissue layer with properties combining those of the ducts, connective tissue, and fat that compose breast tissue. Tissue layer geometries, i.e. thicknesses and volumes, are taken or inferred from literature [5-7]. See Table S1 in Appendix I.

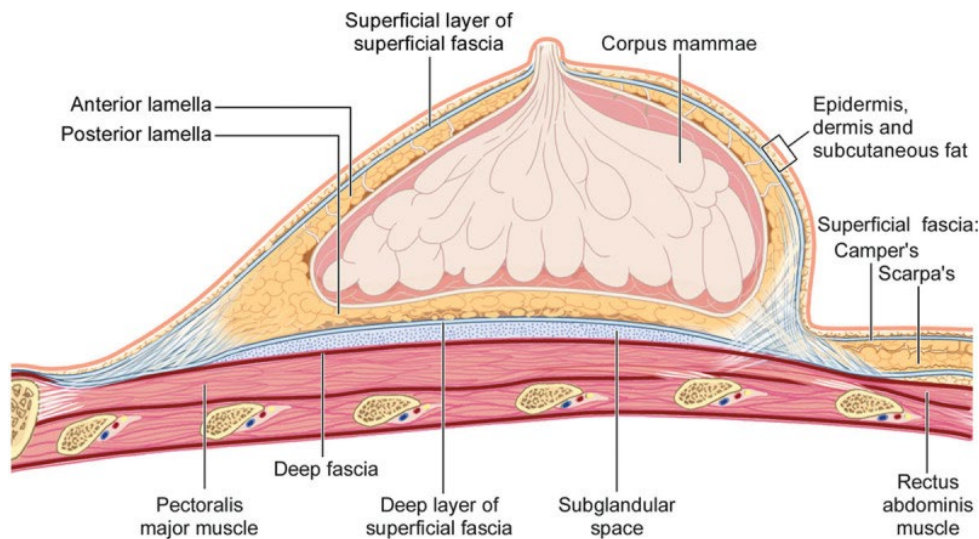


Figure 1: Sagittal view of breast in supine position. Note that most of the breast is made up of fat and specialized breast tissue, both of which are removed entirely during a mastectomy. [8]

In a total mastectomy, the entirety of breast tissue is removed in order to ensure existing tumors and potentially tumorigenic tissues are eradicated. Whether some of the anterior lamina fat (in the anterior lamella) is preserved is up to the individual surgeon [9]. For our study, we are assuming the removal of all tissue within the boundary of the superficial fascia [10]. For breast reconstruction post-mastectomy, we are assuming the implant will completely replace the volume of the excised breast tissue.

We assume the model to be in steady state because heat loss to the environment is a process that is constantly ongoing and is a key component of homeostasis, thus it is fairly constant over time (as long as external conditions are relatively unchanged). The metabolic heat generation term is assumed to be uniform within each of the tissue layers since each layer is assumed to be homogenous. Metabolic heat generation terms will be included for all layers except clothing and

breast implant, since these are not heat-producing materials. We will assume the inner boundary is at a constant (human body) temperature because it is adjacent to the body's core.

3.2 Schematic

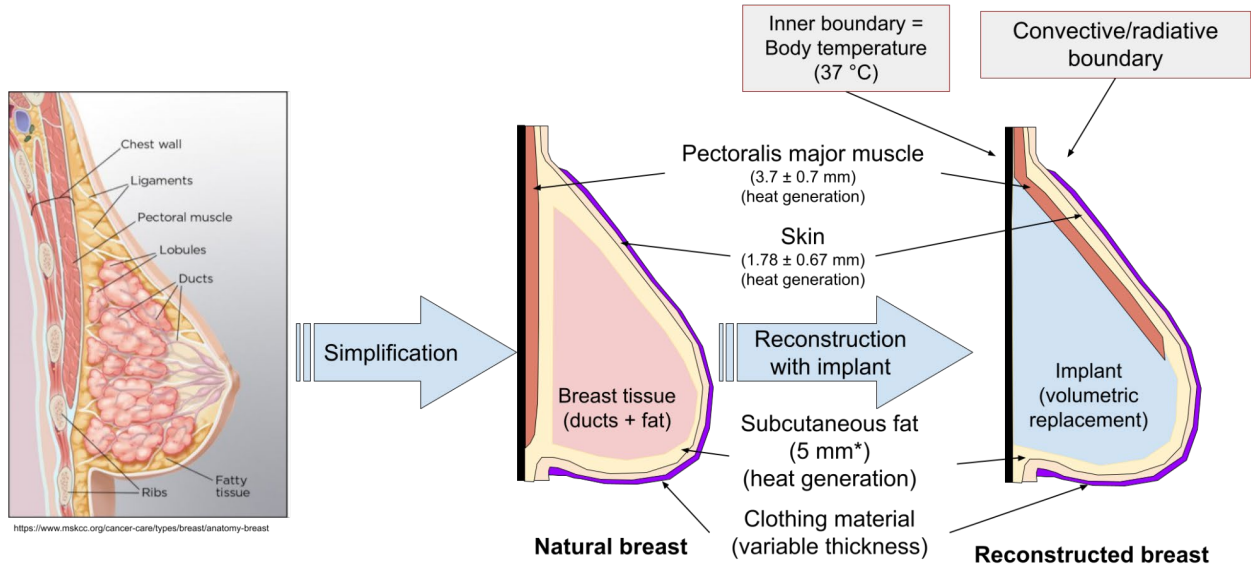


Figure 2: Schematic of natural and reconstructed breast model. The complexity of physiological breasts is simplified to be separate distinct tissue layers. Each tissue layer is treated as being homogenous throughout the layer. The natural breast includes muscle, breast tissue, subcutaneous fat, skin, and clothing layers. The reconstructed breast includes implant, muscle, subcutaneous fat, skin, and clothing layers.

The geometry - representing the “average” breast - was obtained from the Regensburg Breast Shape Model (RBSM), a statistics-based model of the female breasts [11]. This study was published in January 2022 and represents the current state of breast shape modeling. See Appendix II for step-by-step details on how the geometry was created, preprocessed, and imported into COMSOL.

In the reconstructed breast, the muscle layer that was once below the breast tissue is placed over the implant to model a submuscular implant placement. This is a common procedure done after breast cancer patients undergo mastectomies since there is often not enough tissue left for a subglandular implant placement [12].

3.3 Governing Equations

The bioheat equation in three dimensions can be used to model this problem [13]. Since the problem is assumed to be steady state, the transient term is ignored. Therefore, the governing equation reduces to (Equation 1):

$$k\nabla^2 T + \rho_b c_b \dot{V}_b (T_a - T) + Q_{met} = 0 \quad (1)$$

where k is the thermal conductivity of the tissue, ρ_b is the density of the blood, c_b is the specific heat of the blood, \dot{V}_b is the volumetric flow rate of the blood, T_a is the blood temperature, and Q_{met} is metabolic heat generation of the tissue.

3.4 Boundary Conditions

3.4.1 Inside Body Boundary Condition:

The inner (chest side) boundary of the domain will be given a constant temperature of 37°C , which is equivalent to the standard human body internal temperature. This profile is curved to represent the outside surface of the ribcage.

3.4.2 Skin Boundary Condition:

This study will ignore the respiratory and evaporative forms of bodily heat loss since they are irrelevant or negligible for our model. There is no mass transfer, resulting in no respiratory and evaporative heat loss and conductive heat loss is negligible in air. We will consider only convective and radiative heat loss. The outside air is assumed to be 20°C , with airflow relative to the body of 2 m/s . This simulates conditions for a person ranging from sitting in an air-conditioned room to taking a walk in the park on a nice day. We assume a constant convective coefficient value since the literature finds constant coefficients for the entire chest area [14].

The convective heat transfer value for air is given by the equation:

$$h_c = \sqrt{a_{nat} * \sqrt{T_{skin} - T_\infty} + a_{frc} * v_a + a_{mix}} \quad (2)$$

where h_c is the convective heat transfer coefficient in $\text{W/m}^2\text{K}$ at the surface of the body, T_{skin} and T_∞ are the temperatures of the skin and air (in Celcius or Kelvin), v_a is the relative velocity of the air relative to the body in m/s , and a_{nat} , a_{frc} , and a_{mix} are coefficients for the natural convection, forced convection and mixed convection, respectively. The coefficients for the chest area are experimentally calculated to be $a_{nat}=-0.0319$, $a_{frc}=298.69$, $a_{mix}=-19.172$. [14] We set skin temperature to $T = 35^\circ\text{C}$ [15], $T_\infty = 20^\circ\text{C}$.

$$h_c(v = 2 \frac{\text{m}}{\text{s}}) = 24.04 \frac{\text{W}}{\text{m}^2\text{K}} \quad (3)$$

The radiative heat loss is given by:

$$Q'' = \sigma\epsilon(T^4 - T_\infty^4) \quad (4)$$

Since the difference in temperature between the clothes and the air is relatively small, the above equation will be linearized with respect to the temperature difference with a constant of proportionality, h_{rad} , thus becoming:

$$Q'' = h_{rad}(T - T_{\infty}) \quad (5)$$

In order to solve for h_{rad} , we equate the radiation Q'' with the approximated equation. All temperatures are calculated in Kelvin. We again set skin temperature to $T = 35^{\circ}C$, $T_{\infty} = 20^{\circ}C$, and $\epsilon = 0.98$ [21], and the Stefan-Boltzmann constant $\sigma = 5.67 * 10^{-8}$ and solve for h_{rad} as follows:

$$h_{rad}(T - T_{\infty}) = \sigma\epsilon(T^4 - T_{\infty}^4) \quad (6)$$

$$h_{rad} = \sigma\epsilon \frac{T^4 - T_{\infty}^4}{T - T_{\infty}} = 6.03 \frac{W}{m^2K} \quad (7)$$

Thus the total convection value for the exposed skin is:

$$h_{total} = h_c + h_{rad} = 32.23 \frac{W}{m^2K} \quad (8)$$

$$h_c = f(v, f_{cl})$$

3.4.3 Clothing Boundary Condition:

We apply the same process to find heat transfer from the clothes, albeit with a slightly different formula that accounts for the clothing area factor [17]. The equation for convection is thus:

$$Q'' = f_{cl}h_c(T - T_{\infty}) = h_{c,eff}(T - T_{\infty}) \quad (9)$$

where f_{cl} is the clothing area factor, h_c is the convection coefficient, and $h_{c,eff}$ is the effective convective heat transfer coefficient. For clothing, h and f values are calculated as follows:

$$h_c = 12.1 * v_a^{0.5} \quad (10)$$

$$h_c(v = 2 \frac{m}{s}) = 17.1 \frac{W}{m^2K} \quad (11)$$

$$f_{cl} = 1.05 + 0.1 * I_{cl} \quad (12)$$

where I_{cl} is the thermal insulation of the clothing. For a typical bra, $I_{cl} = 0.3$.

$$f_{cl} = 1.08 \quad (13)$$

$$h_{c,eff} = h_c * f_{cl} = 18.48 \frac{W}{m^2K} \quad (14)$$

For radiation, we apply the same equation balance as the skin boundary condition (15). We let the temperature of the surface of the clothes be halfway between skin temperature [15] and ambient temperature $= \frac{35-20}{2} = 27.5^{\circ}C$. The emissivity of clothes is very similar to a black body and can be approximated to 1, and the radiative heat transfer coefficient can be determined (16). We can use the combined convective and radiative coefficient values (17) to approximate the heat transfer in the clothing boundary.

$$h_{rad}(T - T_{\infty}) = \sigma\epsilon f_{cl}(T^4 - T_{\infty}^4) \quad (15)$$

$$h_{rad} = \sigma\epsilon \frac{(T^4 - T_{\infty}^4)}{T - T_{\infty}} = 5.93 \frac{W}{m^2K} \quad (16)$$

$$h_{total} = h_{c,eff} + h_{rad} = 24.41 \frac{W}{m^2K} \quad (17)$$

4. RESULTS

4.1 Mesh Convergence Analysis

Mesh convergence analysis was performed using nine points at the clothing, skin, and subcutaneous fat layers at approximately mid-breast (plane shown in Figure 3a). Three points were chosen at each layer at approximately mid-thickness of the respective layer (Figure 3b). We evaluated the convergence of temperature at each of these points as the mesh was made finer by decreasing element size.

We found that the temperature at each point converged at solution 4 or 5, which correspond to “fine” and “finer” meshes. At these levels of mesh fineness, temperature varied by only about 0.001 °C, which is more than enough precision needed for our analyses. See Figure 4 for a representative plot. We concluded that the “finer” mesh fineness for our model is the best choice that is both precise enough and computationally efficient. See Appendix III, Table S3 for specific parameters used, including maximum and minimum element sizes.

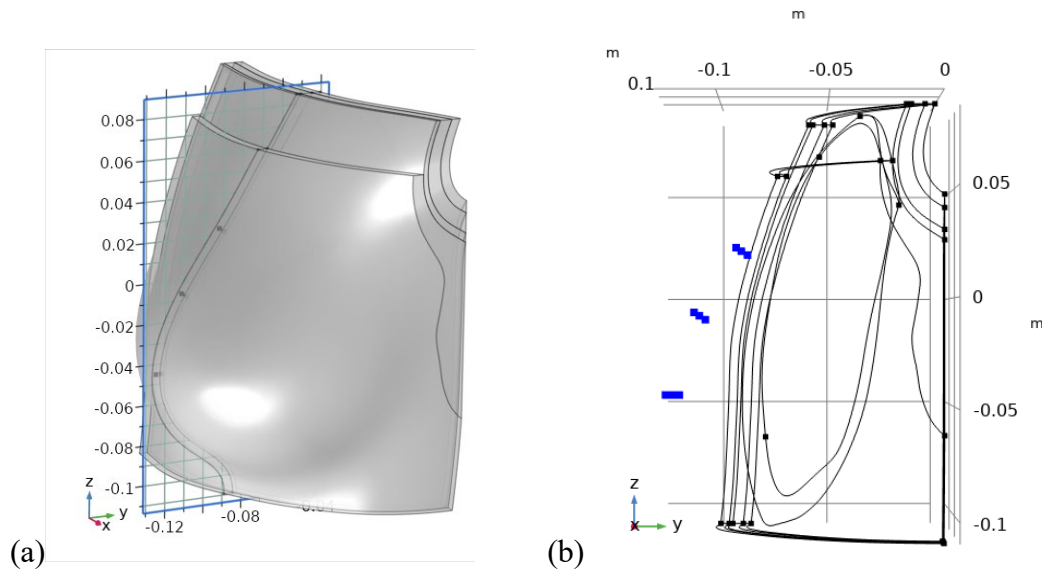


Figure 3: Points chosen for mesh study. The points highlighted in blue indicate the coordinates chosen for mesh convergence study. Three different points were chosen for each of the clothing, skin, and subcutaneous fat layers. Each point is at mid-thickness of its respective layer.

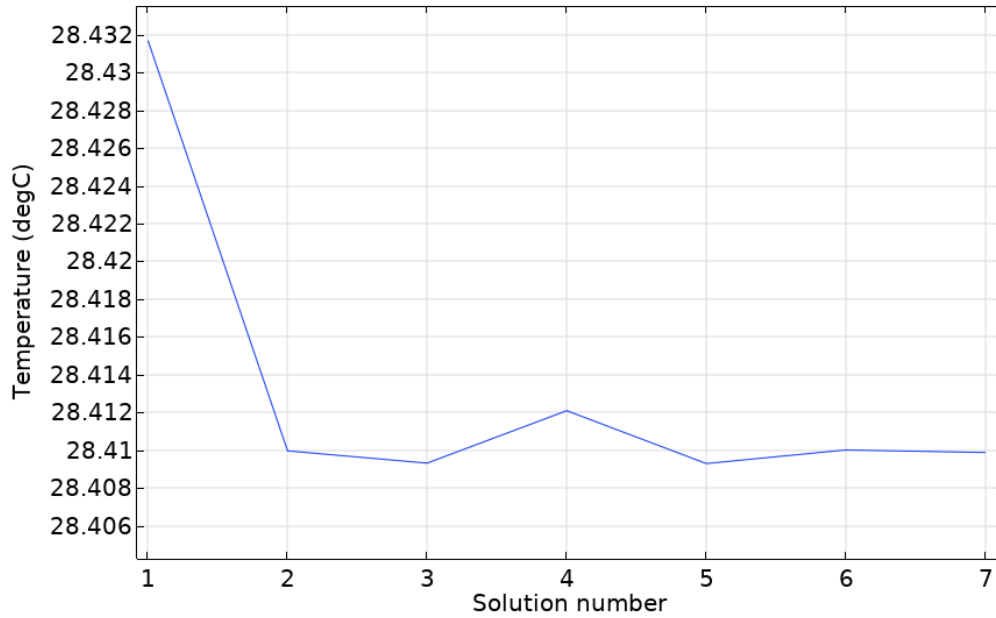


Figure 4: Mesh convergence around solution number 5 (“finer” mesh). This is a representative plot, as the temperatures at different points span a wide range and cannot be shown all at once with the necessary y-axis granularity.

4.2 Objective Function

The objective function for this project aims to keep the temperature at the locations of the temperature receptors in the body within an optimal comfort zone. The function can be expressed as follows:

$$|T_i - T_n| \leq 0.5 * R_{opt} \quad (18)$$

T_i and T_n represent the average temperatures at the depth of the temperature receptors for the reconstructed breast and natural breast cases, respectively. R_{opt} is the range of optimal temperature in order for a person to feel comfortable.

Further analysis will include a 1D plot displaying average temperature at the anterior surface of the muscle layer, where thermoreceptors are located [18,19], versus thermal resistivity of the clothing layer in order to understand what kind of clothing properties are necessary to prevent a patient from feeling cold at their breasts.

4.3 Temperature Distribution

The figures below show only the muscle layer (where temperature-responsive nociceptors are located).. With the “default” bra layer thickness of 4 mm, the natural breast model returned a muscle layer average temperature of 36.885 °C while the reconstructed breast model returned a muscle layer average temperature of 36.142 °C, a difference of 0.743 °C.

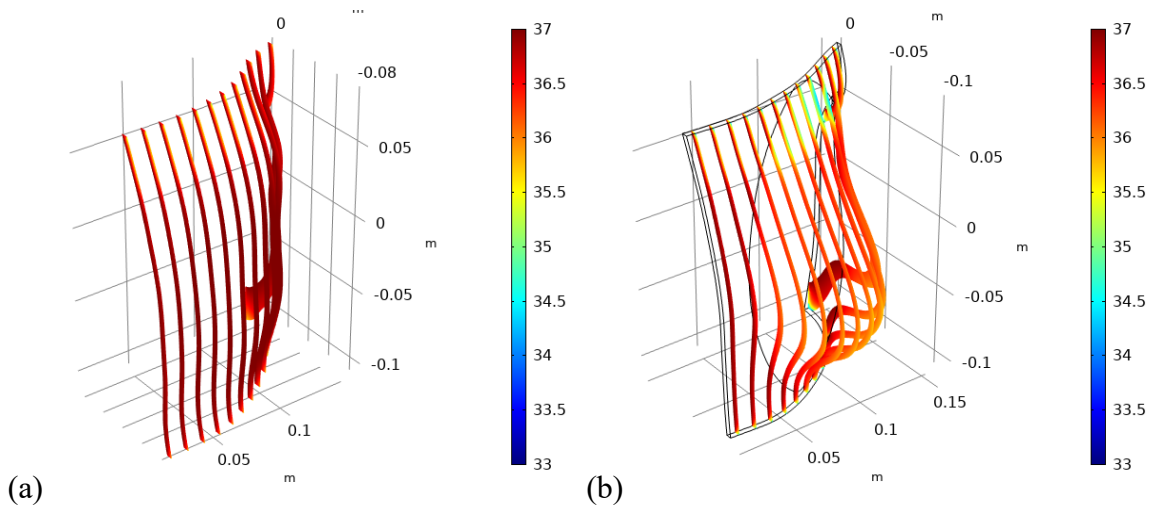


Figure 5: Temperature distribution at muscle layer. The natural breast has the muscle under the breast tissue (a) while the reconstructed breast has the muscle over the implant (b). The natural breast model is shown to be warmer at the muscle layer compared to the reconstructed breast model. The difference between the average temperatures of the muscle layers was calculated to be 0.743 °C.

4.4 Sensitivity Analysis

Sensitivity analysis for material and tissue properties were performed with property value ranges $\pm 20\%$ of the selected literature values. The h_c value was set to a range of reasonable values, roughly $\pm 100\%$ of the set value. The output value evaluated was the average temperature at the muscle layer surface. Convective heat coefficient (h_c), density of breast tissue (ρ_{breast}), specific heat of breast tissue (Cp_{breast}), and thermal conductivity of breast tissue (k_{breast}) were evaluated for the natural breast model. Convective heat coefficient (h_c), thermal conductivity of implant (k_{pdms}), and thermal conductivity of bra material (k_{bra}) were evaluated for the reconstructed breast model. The temperature range seen with changes of parameter values are negligible for most of the parameters. The exception appears to be the convective heat coefficient, which still only affects output value by about $\pm 2\%$ (Fig. 6). The h_c value was varied a lot more than the property values since different external conditions can easily yield vastly different convective coefficients because of its high dependence on wind speed. Practically, the wind speed has much to do with the comfort level that a person feels so it is reasonable that the output temperature would vary highly with h_c .

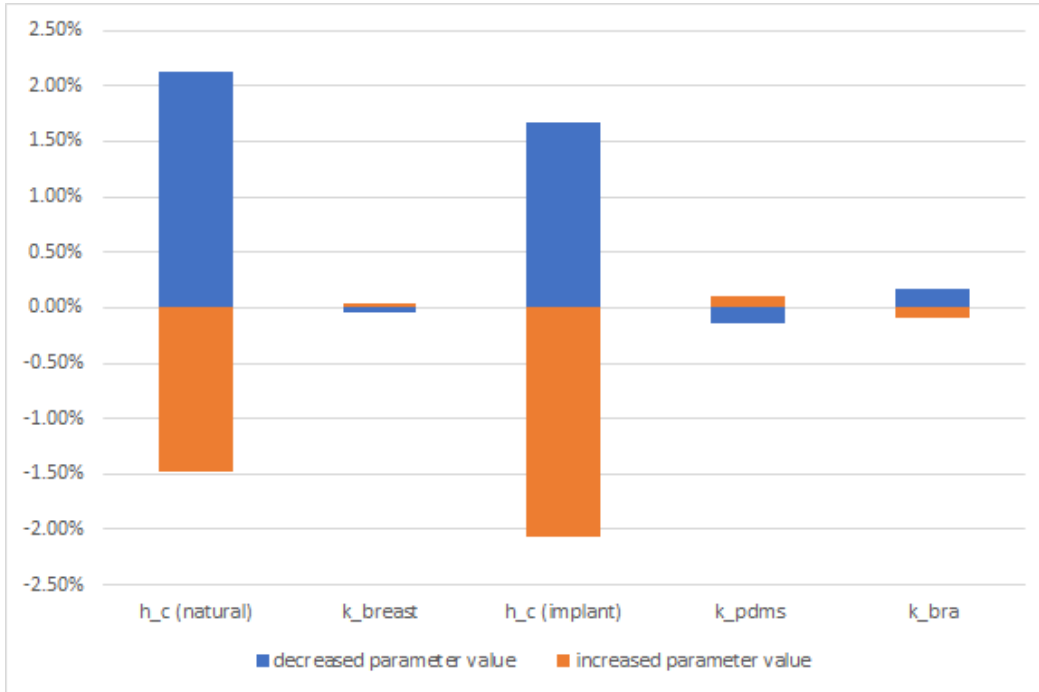
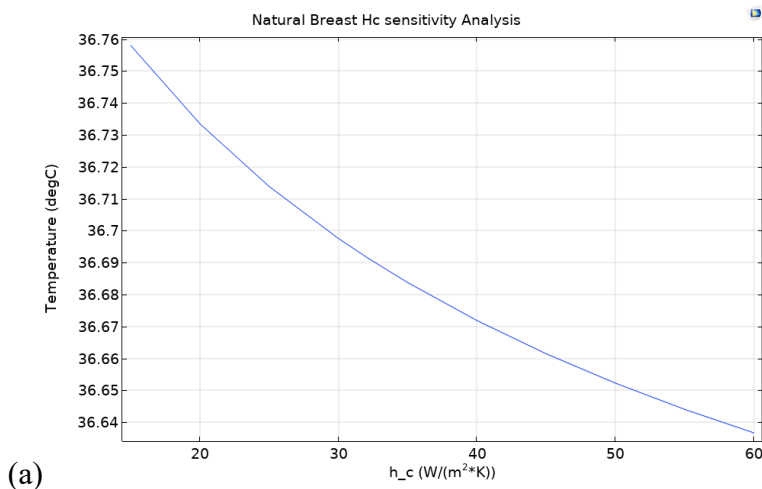


Figure 6: Sensitivity analysis regarding the effect of varying parameters against average skin surface temperature, most parameters have little effect on the temperature. However, varying the h_c value led to a much more significant change in temperature. This is expected since a person should feel colder when there is a higher heat flux into the environment, corresponding with a higher h_c . Graphs showing those particular sensitivity analyses are shown below.



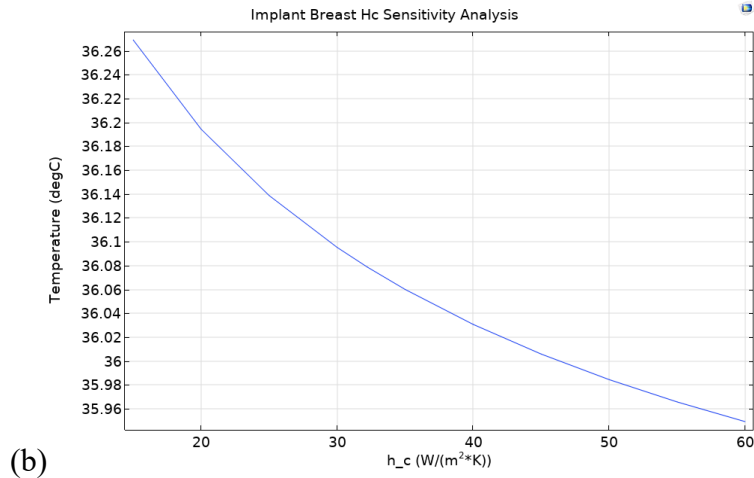


Figure 7: These figures show the sensitivity of average muscle surface temperature to the h_c value. For low h_c values, the natural breast is roughly 0.5 °C higher than the reconstructed. Since both values are fairly high, this is still a comfortable arrangement for both cases. However, for higher h_c values, the difference increases to roughly 0.67 °C (~36.63 vs 35.97°C). At these lower temperatures, this difference between these is much more significant and the post-mastectomy patient will feel a lot colder. The h_c value is highly dependent on wind speed so going out in windy conditions, especially at low temperatures, can prove very discomforting for patients with implants.

4.5 Validation

The model was validated using a study by de Souza et. al. [20] which found an expression for the average temperature of natural breasts T_{avg} , as a function of the room temperature T_{room} and the core temperature T_{core} , all in Celsius:

$$T_{avg} = 12.405 + (T_{core} * 0.548) + (T_{room} * 0.100) \quad (19)$$

This equation allows for the estimation of average breast temperature to validate the model's accuracy in both overall trends and specific temperature points. Note that this equation applies to the natural model only, and similar equations for reconstructed breasts could not be found in the literature. However, validation of the natural model should be sufficient because it differs from the reconstructed breast model only in some layer materials and orientations.

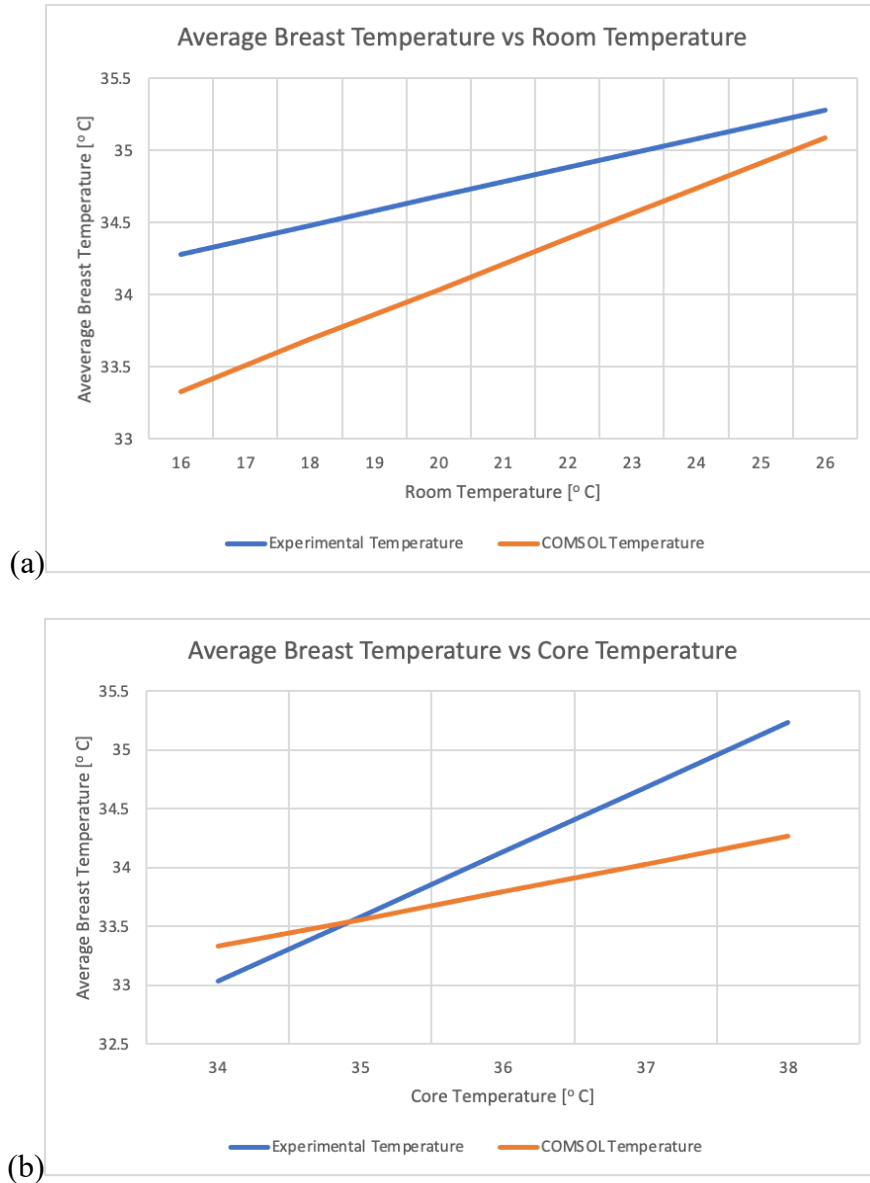


Figure 7: The average breast temperature computed by COMSOL shows reasonable agreement with the experimentally predicted temperature as room temperature varies (a) or as core temperature varies (b).

Figure 7a shows the variation in the average breast temperature with variation in room temperature and Figure 7b shows the variation in the average breast temperature with variation in core temperature. The room and core temperatures ranges shown in Figure 7 are consistent with the experimental data ranges for these parameters used to develop Equation 19. To calculate the error between the COMSOL temperature and the predicted temperature a simple percent difference using the predicted temperature as a baseline was used. The COMSOL model agrees quite well with the temperature values predicted (Equation 19) in their overall trends. With regard to specific points, the model has an average error with respect to the equation of 4.15%

when room temperature is varied and 3.51% when core temperature is varied. This corresponds to a temperature difference of about 1 °C, which might be significant if it corresponded to a variation in core temperature but is reasonable given that the breasts are offset from the core of the body. Overall, the agreement between the models is good, and considering that the study that produced Equation 19 might have had flaws the model can be considered sufficiently validated.

4.6 Varying Design Parameters

We considered multiple fabric materials and thicknesses to inform our design of an insulating bra. To compare the different fabric materials, we ran the model using a bra layer thickness of 4 mm. Wool material resulted in the highest muscle temperature in the reconstructed breast model, at 36.229 °C. Cotton and bamboo followed closely, both at 36.142 °C.

Table 1: Muscle temperature in model with various fabric materials. Wool appears to provide the most insulation, bringing the muscle temperature to 36.229 °C, compared to the natural breast model muscle temperature of 36.885 °C

| | | cotton | neoprene | wool | Lycra | bamboo |
|--|------------------------------|--------|----------|--------|--------|--------|
| Reconstructed Breast Model Muscle Temperature (degC) | | 36.142 | 36.002 | 36.229 | 35.965 | 36.142 |
| Material Properties | Density (g/cm ³) | 0.25 | 0.181 | 0.25 | 0.22 | 0.25 |
| | Specific Heat (J/gC) | 1.34 | 1.117 | 1.72 | 0.976 | 1.25 |
| | Thermal Conductivity (W/mK) | 0.04 | 0.054 | 0.033 | 0.0585 | 0.04 |

To determine the best fabric thickness, we ran the model using cotton as the material and bra layer thicknesses 2 mm to 10 mm. We were unable to generate geometries with bra layer thicknesses larger than 10 mm due to CAD modeling issues. Within the implemented range, the average muscle temperature in the reconstructed breast model did not reach the temperature seen in the natural breast model.

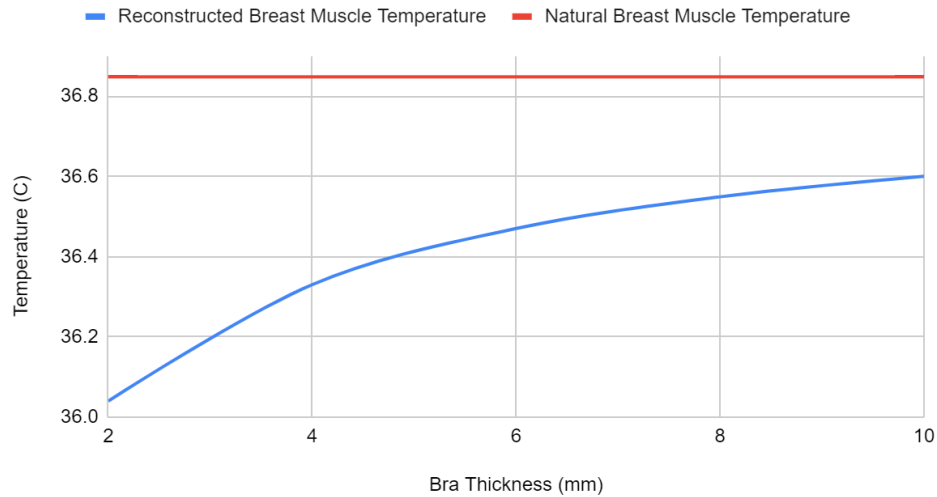


Figure 8: Bra layer thickness versus average muscle temperature. Muscle temperature in the reconstructed breast model ranges from 36.040 °C at 2 mm bra thickness to 36.600 °C at 10 mm bra thickness.

5. DISCUSSION

The objective of this study was to determine the fabric material and thickness required for an insulating bra that will prevent patients from experiencing excessive heat loss and the associated cold/pain sensations in their breasts at cool room temperature. The model suggests that wool fabric provides the best insulation, followed closely by cotton and bamboo. However, we used cotton as our material of choice due to its affordability, availability, and comfort in comparison to the other materials. Within the tested bra layer thickness range of 2 - 10 mm, the average muscle temperature in the reconstructed breast model did not reach the temperature seen in the natural breast model. The results also suggest that thickening the clothing layer has diminishing returns. The results of the model show that, with the chosen material and thicknesses, a cotton bra of 10 mm thickness does not provide enough insulation to keep a mastectomy patient's breasts at the temperature of natural breasts.

6. CONCLUSION

This study sought to better understand how much heat loss in the chest occurs in post-mastectomy breast reconstruction patients compared to those with natural breasts through modeling. We performed heat transfer analysis with geometry based on a representation of the statistical average breast. The model was validated with a study that described an expression for the average temperature of natural breasts as a function of the room temperature and the core

temperature; values computed in the model were acceptably close to values calculated using the described expression.

We found a temperature difference of 0.743 °C in the muscle layer between natural and reconstructed breast models. Using this information, we sought to determine ideal thicknesses and material to inform design of insulating bras for breast-reconstruction patients. The results suggest that a bra designed with cotton fabric of 10mm thickness is unable to insulate the breast to maintain the same temperature as the natural breasts.

Design Recommendations

Our study demonstrates that, for insulation of reconstructed breasts, material thickness must be at least 10 mm. The results also suggest, however, that there are diminishing returns with increasing thickness. While wool provides better insulation than the other materials, cotton is considered to be the fabric of choice. This is because cotton follows closely behind wool in terms of insulation and is generally the most economical and comfortable fabric.

Using this information, future efforts to design bras for mastectomy patients should consider increased padding thickness, using blended fabric materials, including multiple layers of different fabrics, or including an active heating element in the bra.

APPENDIX I: Model Input Parameters

Tissue layer geometries, i.e. thicknesses and volumes, are taken or inferred from literature (10–12), shown in Table S1.

Table S1: Layer thicknesses and sources.

| Layer | Thickness (mm) | Source |
|------------------|----------------|----------------------|
| Clothing | Variable | - |
| Skin | 1.78 ± 0.67 mm | Coltman et al., 2017 |
| Subcutaneous fat | 5 mm | Canturk et al., 2021 |
| Muscle | 3.7 ± 0.7 mm | Ishii et al., 2018 |

All parameter values for tissue and boundary properties were obtained from a database with values compiled from literature, directly from literature, or calculated values derived from literature. Values, assumptions, notes on calculations, and sources are in Table S2 in the Appendix.

The “breast tissue” layer is the combination of breast fat, breast glands, and connective tissue. The parameter values for breast tissue are calculated as weighted averages.

$$C_{p,eff} = \frac{\sum_i \epsilon_i \rho_i C_{p(i)}}{\sum_i \epsilon_i \rho_i} \quad [16]$$

$$\rho_{eff} = \left(\sum_i \frac{\text{mass fraction}}{\rho_i} \right)^{-1} \quad [21]$$

Table S2: Input parameters used in the model.

| Property | Material | Name | Value Expression | Notes |
|----------|----------------------------|-----------------|--------------------------|--|
| Density | Air | ρ_{air} | 1.13[kg/m ³] | |
| | Breast Tissue (calculated) | ρ_{breast} | 1015[kg/m ³] | Calculated as average of breast gland, fat, connective tissue values weighted by volume fraction |
| | Fat (general) | ρ_{fat} | 911[kg/m ³] | |
| | Muscle | ρ_{muscle} | 1090[kg/m ³] | |
| | Skin | ρ_{skin} | 1109[kg/m ³] | |

| | | | | |
|-----------------------------|----------------------------|-----------------|--------------------------|--|
| | Blood Perfusion Rate: | ρ_{blood} | 1050[kg/m ³] | |
| | Water | ρ_{water} | 994[kg/m ³] | |
| | Cotton | ρ_{cotton} | .25 [kg/m ³] | Experimental data |
| Specific Heat | Air | Cp_{air} | 1005[J/kg/degC] | |
| | Breast Tissue (calculated) | Cp_{breast} | 2700[J/kg/degC] | Calculated as average of breast gland, fat, connective tissue values weighted by volume fraction |
| | Fat (general) | Cp_{fat} | 2348[J/kg/degC] | |
| | Muscle | Cp_{muscle} | 3421[J/kg/degC] | |
| | Skin | Cp_{skin} | 3391[J/kg/degC] | |
| | Blood Perfusion Rate: | Cp_{blood} | 3617[J/kg/degC] | |
| | Water | Cp_{water} | 4178[J/kg/degC] | |
| | Cotton [22] | Cp_{cotton} | 1340 [J/kg/degC] | |
| Thermal Conductivity | Air | k_{air} | 0.03[W/m/degC] | |
| | Breast Tissue (calculated) | k_{breast} | 0.31[W/m/degC] | Calculated as average of breast gland, fat, connective tissue values weighted by volume fraction |
| | Fat (all) | k_{fat} | 0.21[W/m/degC] | |
| | Muscle | k_{muscle} | 0.49[W/m/degC] | |
| | Skin | k_{skin} | 0.37[W/m/degC] | |
| | Blood Perfusion Rate: | k_{blood} | 0.52[W/m/degC] | |
| | Water | k_{water} | 0.6[W/m/degC] | |
| | Cotton [23] | k_{cotton} | .04 [W/m/degC] | |
| | Lycra [24] | k_{lycra} | 0.0585 [W/m/degC] | |
| | Bamboo [25] | k_{bamboo} | 0.04 [W/m/degC] | |

| | | | | |
|--|-------------------------------|----------------------|-----------------------------------|--|
| Perfusion Rate (per unit mass tissue) | Breast Fat | $perf_{breast\ fat}$ | 47[ml/min/kg] | |
| | Breast Tissue (calculated) | $perf_{breast}$ | 100[ml/min/kg] | Calculated as average of breast gland, fat, connective tissue values weighted by volume fraction |
| | Fat (general) | $perf_{fat}$ | 33[ml/min/kg] | |
| | Muscle | $perf_{muscle}$ | 37[ml/min/kg] | |
| | Skin | $perf_{skin}$ | 106[ml/min/kg] | |
| Metabolic Heat Generation (per unit mass) | Breast Fat | $Qm_{breast\ fat}$ | $0.73[W/kg]*\rho_{fat}$ | |
| | Breast Tissue (calculated) | Qm_{breast} | 1.9[W/kg] | Calculated as average of breast gland, fat, connective tissue values weighted by volume fraction |
| | Fat (general) | Qm_{fat} | $0.51[W/kg]*\rho_{fat}$ | |
| | Muscle | Qm_{muscle} | $0.91[W/kg]*\rho_{muscle}$ | |
| | Skin | Qm_{skin} | $1.65[W/kg]*\rho_{skin}$ | |
| Blood Perfusion Rate (per unit volume tissue) | Breast Fat | $omg_{breast\ fat}$ | $perf_{breast\ fat} * \rho_{fat}$ | |
| | Breast Tissue (calculated) | omg_{breast} | $perf_{breast} * \rho_{breast}$ | Calculated as average of breast gland, fat, connective tissue values weighted by volume fraction |
| | Fat (general) | omg_{fat} | $perf_{fat} * \rho_{fat}$ | |
| | Muscle | omg_{muscle} | $perf_{muscle} * \rho_{muscle}$ | |
| | Skin | omg_{skin} | $perf_{skin} * \rho_{skin}$ | |

Values of parameters were sourced from the Zurich43 IT'IS Foundation [16] unless noted otherwise.

APPENDIX II: Generation of Breast Geometry

Using the Scalismo Viewer provided by the study authors, the geometry in Figure S1 was created by taking the mean value of all property options. This represents the “average” breast from the spectrum generated by the 110 breast scans taken in the RBSM study. The following steps were taken to create the geometries analyzed above:

1. Open the Regensburg Breast Shape Model using the Scalismo Viewer and set all parameters to the mean value. Save the geometry as a .STL file.
2. Open the .STL file in Fusion and create the layers and limit the model boundaries to the region of interest. Export as a .IGS file.
3. Open the .IGS file in Spaceclaim and use the applicable tools in the “Prepare” and “Repair” tabs to clean the geometry. Save as a .X_T file.
4. Import into COMSOL using the default geometry import options.

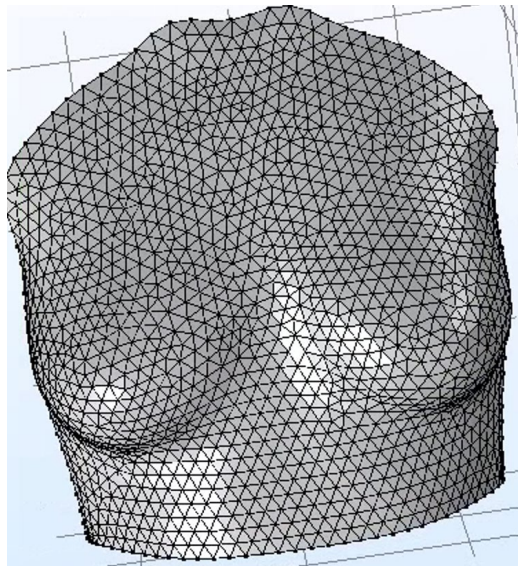


Figure S1: Imported breast geometry represented the statistical average of over 90 scans of women’s breasts. This geometry involves minimal simplifications and introduces less error than a “hand-drawn” 3D or 2D breast.

APPENDIX III: Solution Strategy

```

----- Dependent Variables 1 in Study 1/Solution 1 (sol1) ----->
<----- Stationary Solver 1 in Study 1/Solution 1 (sol1) ----->
Started at May 10, 2022 9:54:26 PM.
Linear solver
Number of degrees of freedom solved for: 312012 (plus 198926 internal DOFs).
Symmetric matrices found.
Scales for dependent variables:
Temperature (compl.T2): 2.9e+02
Orthonormal null-space function used.
Iter   SolEst   Damping   Stepsize #Res #Jac #Sol LinIt   LinErr   LinRes
  1     0.047   1.0000000   0.047   1   1   1   2   0.00095  7.3e-05
Solution time: 9 s.
Physical memory: 2.52 GB
Virtual memory: 2.85 GB
Ended at May 10, 2022 9:54:35 PM.
----- Stationary Solver 1 in Study 1/Solution 1 (sol1) ----->

```

Figure S2: COMSOL runtime and memory used.

Computational Method:

Linear GMRES solver was used. Relative tolerance was set at the default of 0.001.

Mesh convergence analysis was performed using nine points at the clothing, skin, and subcutaneous fat layers at approximately mid-breast (plane shown in Figure 3a). Three points were chosen at each layer at approximately mid-thickness of the respective layer (Figure 3b). We evaluated the convergence of temperature at each of these points with varying mesh fineness of parameter combinations shown in Table S3. Tetrahedral elements were used for the entire mesh.

Table S3: Mesh convergence analysis mesh parameters. Each mesh size fineness was defined by a combination of parameters.

| | Coarser | Coarse | Normal | Fine | Finer | Extra fine |
|---------------------------------------|---------|---------|---------|---------|----------|------------|
| Solution number (arb) | 1 | 2 | 3 | 4 | 5 | 6 |
| Maximum element size (max_e) | 0.0393 | 0.031 | 0.0207 | 0.0165 | 0.0114 | 0.00723 |
| Minimum element size (min_e) | 0.00826 | 0.00579 | 0.00372 | 0.00207 | 0.000826 | 0.00031 |
| Maximum element growth rate (growR) | 1.7 | 1.6 | 1.5 | 1.45 | 1.4 | 1.35 |
| Curvature factor (ResCurv) | 0.8 | 0.7 | 0.6 | 0.5 | 0.4 | 0.3 |
| Resolution of narrow regions (ResNar) | 0.3 | 0.4 | 0.5 | 0.6 | 0.7 | 0.85 |

The temperatures at different points span a wide range and cannot be shown all at once with the necessary y-axis granularity (Figure S3). Temperature plots for each point closely resembled the representative plot shown in Figure 4, with convergence at solution number 4 (“fine” mesh) or 5 (“finer” mesh).

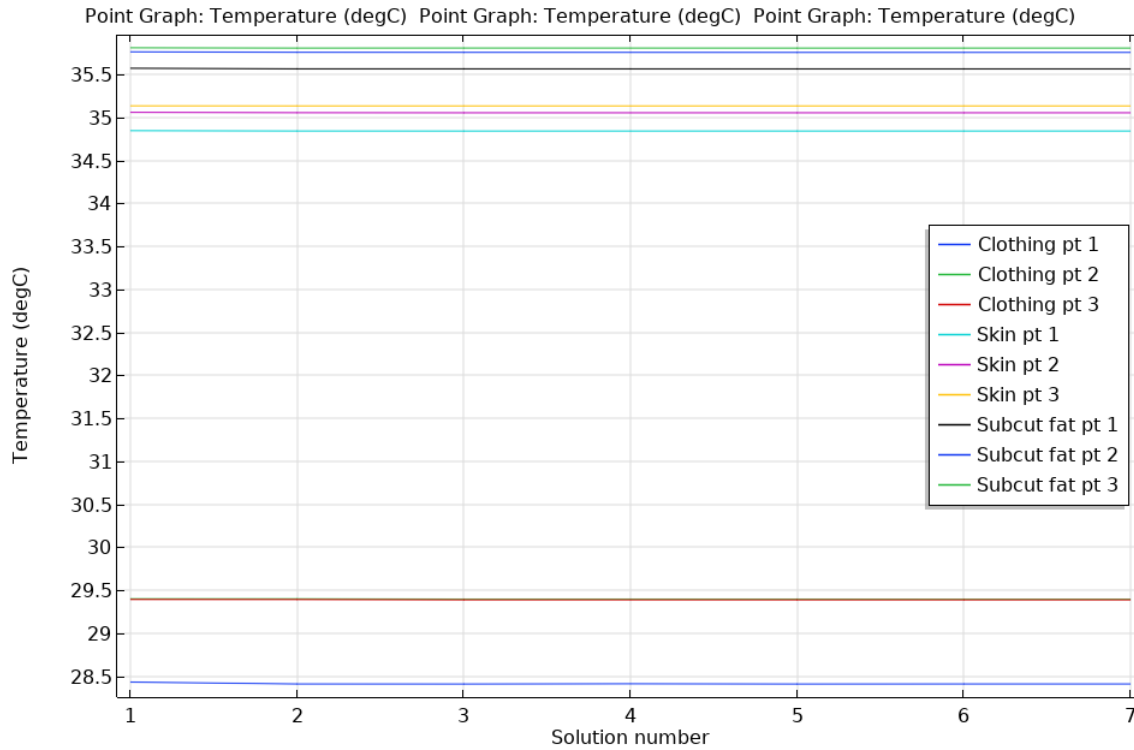
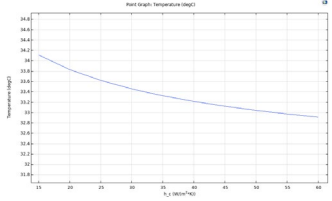
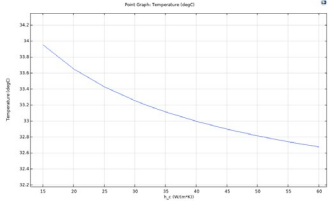
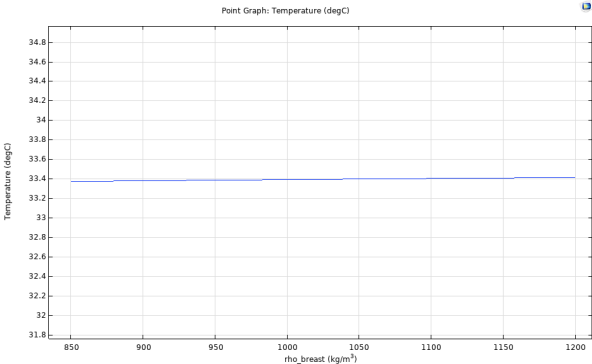
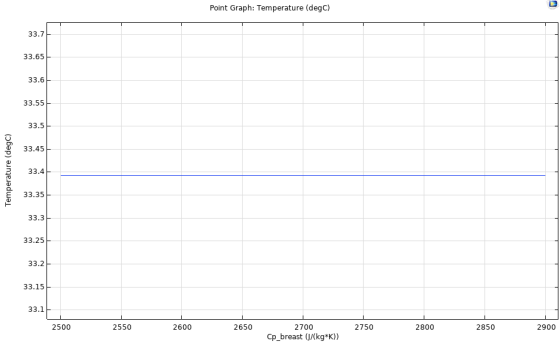
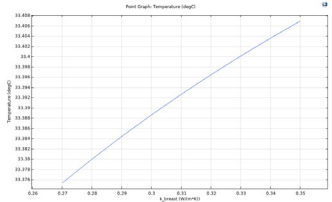
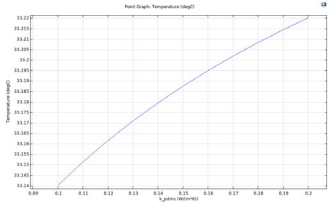
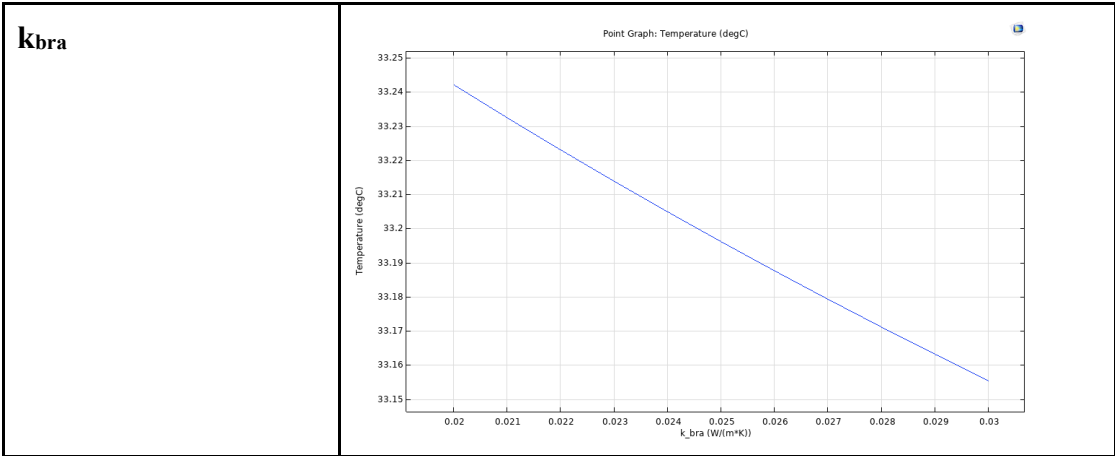


Figure S3: Temperature at all points in mesh convergence analysis. Temperatures vary widely and so this plot does not have the necessary y-axis granularity to assess convergence.

APPENDIX IV: Sensitivity Analysis Plots

Plots differentiated when there is significant difference between the natural and reconstructed breasts

| Parameter Varied | Natural Breast | Reconstructed Breast |
|-----------------------------|---|--|
| h_c |  |  |
| rho_{breast} |  | |
| cp_{breast} |  | |
| k_{breast} |  <p data-bbox="630 1648 776 1686">(k_{breast tissue})</p> |  <p data-bbox="1019 1648 1101 1686">(k_{pdms})</p> |



REFERENCES

- [1] Rüstemova, D., Genc, A., Bora, G., & Tur, B. S. (2017). A thermal dysregulation problem after breast cancer surgery; what could be?. *Medicine*, 96(26), e7027.
<https://doi.org/10.1097/MD.00000000000007027>
- [2] *Mastectomy and Double Mastectomy*. (n.d.). Brigham and Women's Hospital. Retrieved February 18, 2022, from <https://www.brighamandwomens.org/surgery/surgical-oncology/resources/mastectomy>
- [3] Nahabedian, M. Y., & McGibbon, B. M. (1998). Thermal injuries in autogenous tissue breast reconstruction. *British Journal of Plastic Surgery*, 51(8), 599–602.
<https://doi.org/10.1054/bjps.1998.0209>
- [4] Faulkner, H. R., Colwell, A. S., Liao, E. C., Winograd, J. M., & Austen, W. G., Jr (2016). Thermal Injury to Reconstructed Breasts from Commonly Used Warming Devices: A Risk for Reconstructive Failure. *Plastic and reconstructive surgery. Global open*, 4(10), e1033.
<https://doi.org/10.1097/GOX.0000000000001033>
- [5] Ishii N, Ando J, Harao M, Takemae M, Kishi K. Individual difference in pectoralis major muscle thickness and its effect on single-stage breast reconstruction using a tissue expander. *Breast Cancer*. 2018 Jan 1;25(1):68–73.
- [6] Coltman CE, Steele JR, McGhee DE. Effect of aging on breast skin thickness and elasticity: implications for breast support. *Skin Res Technol*. 2017 Aug;23(3):303–11.
- [7] Canturk NZ, Şimşek T, Guler SA. Standard Mastectomy. In: Rezai M, Kocdor MA, Canturk NZ, editors. *Breast Cancer Essentials: Perspectives for Surgeons* [Internet]. Cham: Springer International Publishing; 2021 [cited 2022 Feb 25]. p. 331–47. Available from: https://doi.org/10.1007/978-3-030-73147-2_31
- [8] Rehnke, R. D., Groening, R. M., Van Buskirk, E. R., & Clarke, J. M. (2018). *Anatomy of the superficial fascia system of the breast: a comprehensive theory of breast fascial anatomy*. *Plastic and reconstructive surgery*, 142(5), 1135.
- [9] Chopra S, Rehnke RD, Raghavan V. Implant-based Prepectoral Breast Reconstruction: The Importance of Oncoplastic Plane, its Blood Supply and Assessment Methods. *World J Plast Surg*. 2021 Jan;10(1):108–13.
- [10] Barnea Y, Friedman O. Skin-Sparing and Nipple-Sparing Mastectomies. In: Rezai M, Kocdor MA, Canturk NZ, editors. *Breast Cancer Essentials: Perspectives for Surgeons* [Internet]. Cham: Springer International Publishing; 2021 [cited 2022 Feb 25]. p. 349–58. Available from: https://doi.org/10.1007/978-3-030-73147-2_32

- [11] Maximilian Weiherer, Andreas Eigenberger, Bernhard Egger, Vanessa Brébant, Lukas Prantl, Christoph Palm. Learning the shape of female breasts: an open-access 3D statistical shape model of the female breast built from 110 breast scans. *Vis Comput* (2022).
<https://doi.org/10.1007/s00371-022-02431-3>
- [12] The Plastic Surgery Center [Internet]. <https://www.sacplasticsurgery.com/breast-implant-placement-over-vs-under-the-muscle/>
- [13] Shrestha, Sharmila & Kc, Gokul & Gurung, Dil. (2020). Transient Bioheat Equation in Breast Tissue: Effect of Tumor Size and Location. 10.22606/jaam.2020.51002.
- [14] Jingxian Xu, Agnes Psikuta, Jun Li, Simon Annaheim, René M. Rossi, Evaluation of the convective heat transfer coefficient of human body and its effect on the human thermoregulation predictions, *Building and Environment*, Volume 196, 2021, 107778, ISSN 0360-1323,
<https://doi.org/10.1016/j.buildenv.2021.107778>.
- [15] Bierman W. The Temperature of the Skin Surface. *JAMA*. 1936;106(14):1158–1162.
doi:10.1001/jama.1936.02770140020007
- [16] IT'IS Foundation. Tissue Properties Database V4.1 [Internet]. IT'IS Foundation; 2022 [cited 2022 Mar 11]. Available from: <https://itis.swiss/virtual-population/tissue-properties/downloads/database-v4-1/>
- [17] Ogulata, Tugrul. (2007). The Effect of Thermal Insulation of Clothing on Human Thermal Comfort. *Fibres and Textiles in Eastern Europe*. 15. 67-72.
- [18] Tansey EA, Johnson CD. Recent advances in thermoregulation. *Adv Physiol Educ*. 2015 Sep;39(3):139–48.
- [19] 36.2C: Thermoreception [Internet]. *Biology LibreTexts*. 2018 [cited 2022 Mar 11]. Available from:
[https://bio.libretexts.org/Bookshelves/Introductory_and_General_Biology/Book%3A_General_Biology_\(Boundless\)/36%3A_Sensory_Systems/36.2%3A_Somatosensation/36.2C%3A_Thermoreception](https://bio.libretexts.org/Bookshelves/Introductory_and_General_Biology/Book%3A_General_Biology_(Boundless)/36%3A_Sensory_Systems/36.2%3A_Somatosensation/36.2C%3A_Thermoreception)
- [20] Souza, Gladis Aparecida Galindo Reiserberger de et al. “Reference breast temperature: proposal of an equation.” *Einstein (Sao Paulo, Brazil)* vol. 13,4 (2015): 518-24.
doi:10.1590/S1679-45082015AO3392
- [21] Charlatan,
<https://www.ncbi.nlm.nih.gov/pmc/articles/PMC7688144/#:~:text=Human%20skin%20has%20a,n%20accepted,this%20value%20is%20not%20known>

[22] AmesWeb [Internet]. https://amesweb.info/Materials/Specific_Heat_of_Substances.aspx

[23] U. Gunasekera et al., "Modification of thermal conductivity of cotton fabric using Graphene," *2015 Moratuwa Engineering Research Conference (MERCon)*, 2015, pp. 55-59, doi: 10.1109/MERCon.2015.7112320.

[24] Alibi, H., Fayala, F., Jemni, A., & Zeng, X. (2012). Modeling of Thermal Conductivity of Stretch Knitted Fabrics Using an Optimal Neural Networks System. *Journal of Applied Sciences*, 12(22), 2283–2294. <https://doi.org/10.3923/jas.2012.2283.2294>

[25] Prakash, C., & Ramakrishnan, G. (2013). Effect of blend proportion on thermal behaviour of bamboo knitted fabrics. *Journal of the Textile Institute*, 104(9), 907–913. <https://doi.org/10.1080/00405000.2013.765090>